Evidence for Pb-O Covalency in Tetragonal $PbTiO_3$

Yoshihiro Kuroiwa,* Shinobu Aoyagi, and Akikatsu Sawada
Department of Physics, Okayama University, Okayama 700-8530, Japan

Jimpei Harada
X-ray Research Laboratory, Rigaku Corporation, Akishima, Tokyo 196-8666, Japan

Eiji Nishibori, Masaki Takata, and Makoto Sakata
Department of Applied Physics, Nagoya University, Nagoya 464-8603, Japan
(Received 20 July 2001; published 6 November 2001)

Accurate charge-density distributions of cubic and tetragonal $PbTiO_3$ and $BaTiO_3$ have been obtained by the MEM(maximum entropy method)/Rietveld analysis using synchrotron-radiation powder data. The Pb-O bonds in tetragonal $PbTiO_3$ show rather strong covalency, while those in cubic $PbTiO_3$ are ionic. This is the clear evidence of the Pb-O hybridization in tetragonal $PbTiO_3$, which has been theoretically predicted as a key factor of much larger ferroelectricity of this substance than that of $BaTiO_3$. Tetragonal $PbTiO_3$ forms a layered structure of a two-dimensional covalent-bonding network consisting of the $Ti\text{-}O_5$ pyramid.

DOI: 10.1103/PhysRevLett.87.217601 PACS numbers: 77.84.Dy, 61.10.Nz

Perovskite oxides, which have a chemical formula of ABO_3, are well known for their applications to novel devices [1], such as ferroelectric memories, piezoelectric vibrators, etc. A variety of ferroelectric properties of perovskites can be controlled by a replacement of the A and B cations. Among them, $PbTiO_3$ and $BaTiO_3$ are symbolic examples displaying quite different ferroelectric behavior. Both have a simple cubic structure in the high-temperature paraelectric phase. A phase transition to the tetragonal phase occurs in $PbTiO_3$ and $BaTiO_3$ at 763 and 403 K, respectively. The transition temperature of $PbTiO_3$ is higher than that of $BaTiO_3$, and the spontaneous polarization of $PbTiO_3$ is about 3 times larger than that of $BaTiO_3$ at room temperature [2]. Comparing both the lattice strains in the tetragonal phase at room temperature, the c/a ratio of $PbTiO_3$ is 1.06, whereas that of $BaTiO_3$ is only 1.01, where a and c are the lattice constants [3]. In addition, $BaTiO_3$ is known to have successive phase transitions, from the cubic structure to tetragonal, orthorhombic, and rhombohedral structures at low temperatures.

In the 1990s, theoretical studies by first-principles calculations suggested a specific scenario to give a plausible account of these replacement effects on the ferroelectric properties of perovskites [4–9]. It was pointed out that the hybridization between the Ti $3d$ states and O $2p$ states is essential to the ferroelectric instability in both $PbTiO_3$ and $BaTiO_3$, and that the orbital hybridization exists between the Pb $6s$ state and O $2p$ states to play a crucial role for larger ferroelectricity [5,6] in tetragonal $PbTiO_3$, whereas the interaction between Ba and O is almost ionic in tetragonal $BaTiO_3$. The theoretical prediction can be verified by an x-ray charge-density study on the bonding electron distributions associated with the orbital hybridization. Until now, however, no experimental evidence for the Pb-O orbital hybridization has been reported. In this study, we report a direct experimental evidence for the Pb-O hybridization revealed as the Pb-O covalent bonding electron distribution in the precise charge-density distribution of tetragonal $PbTiO_3$ for the first time.

In order to determine precise electron-density maps by x-ray diffraction, it is essential to collect accurate Bragg integrated intensity data. In this study, high-energy synchrotron x-ray powder-diffraction data were collected for the analyses of both cubic and tetragonal $PbTiO_3$ and $BaTiO_3$. The merits of the experiment are as follows. A powder-diffraction experiment has an advantage to be free from the problems of ferroelectric multidomains. Extinction effects also can be excluded. In addition, high-energy x-rays are efficient to exclude the absorption effect for the specimen such as $PbTiO_3$ consisting of an extremely heavy element, Pb, and a light element, O. The experiments were carried out on the Large Debye-Scherrer Camera installed at BL02B2 in SPring-8. The temperatures were stabilized within 1 K by the N_2 gas flow system. In order to get good counting statistics, an imaging plate was used as a detector. The performance of the camera has been reported elsewhere [10]. A homogeneous granularity of the sample powder, which gives a homogeneous intensity distribution in the Debye-Scherrer powder ring, was achieved by the precipitation method. The powder of $PbTiO_3$ was sealed into a quartz capillary of 0.1 mm in diameter. The wavelength of the incident beam used was 0.41 Å. In these experimental conditions, the factor to be compensated for absorption was only 0.5% for the intensity at $2\theta = 50°$, as was fairly small to be ignored. For the experiment of $BaTiO_3$, a capillary of 0.2 mm in diameter and x-rays of 0.50 Å were adopted.

The electron-density distributions were determined by the MEM/Rietveld technique, which is a combination of the MEM (maximum entropy method) [11] and the

Rietveld refinement [12]. The technique has been successfully applied to the structure studies of fullerene compounds [13–15], intermetallic compounds [16], manganites [17], etc. For instance, Takata *et al.* have succeeded also in observing the orbital order of Mn $3dx^2$-y^2 in the antiferromagnetic state of the manganite, $NdSr_2Mn_2O_7$, revealed in the Mn-O bonding electron distribution associated with $Mn(3dx^2\text{-}y^2)$-$O(2p\sigma)$ orbital hybridization using synchrontron-radiation powder data [17]. These studies have proven that the MEM can derive detailed bonding electron distributions purely from a limited number of diffraction data. The accurate bonding nature could not be easily deduced by only the Rietveld refinement, which assumes a structure model based on an arrangement of free atoms. Therefore, it can be considered that the MEM/Rietveld analysis is a powerful method for a direct observation of change in bonding electron densities in the interatomic region associated with the phase transition. The detail of the present method has been described previously [13–17].

The fitting results of the preliminary Rietveld analyses in the MEM/Reitveld method for 800 and 300 K data of $PbTiO_3$ are shown in Fig. 1. The refined crystal-structure parameters obtained by the Rietveld analyses are listed in Table I. The 51 and 233 independent observed structure factors were derived by the preliminary Rietveld analyses for 800 and 300 K data, respectively, and used in the MEM analyses. The reliability factors (R factors) based on the Bragg intensities, R_I, and the weighted profile, R_{wp}, were 2.35% and 3.74%, respectively, for 800 K data. For 300 K data, R_I was 1.72% and R_{wp} was 2.25%. The MEM analyses were carried out with the unit cell divided into $80 \times 80 \times 80$ and $80 \times 80 \times 84$ pixels for 800 and 300 K, respectively. The volume of one pixel corresponds to about $0.05 \times 0.05 \times 0.05$ Å^3. The reliable factor based on the structure factors, R_F, was 1.02% and 0.99% for the final MEM charge density at 800 and 300 K, respectively.

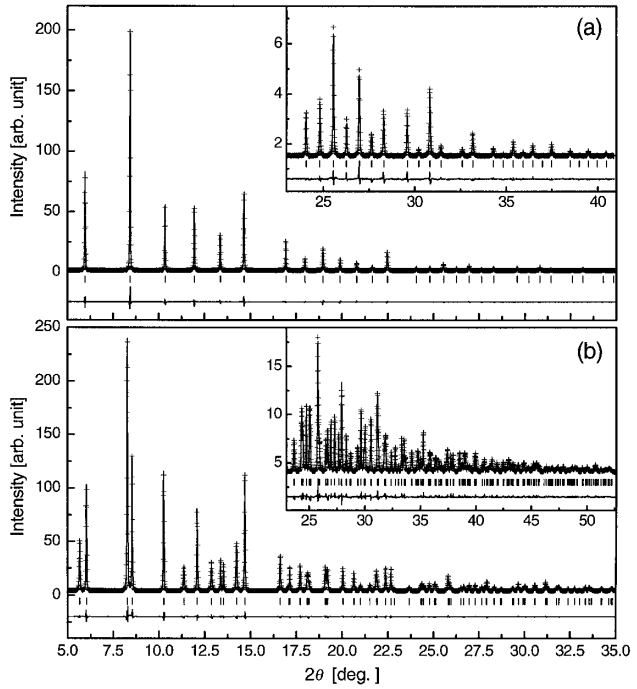

FIG. 1. Rietveld fitting for $PbTiO_3$ at (a) 800 K (cubic phase) and (b) 300 K (tetragonal phase). The data up to 42.0° and 52.6° in 2θ, which corresponds to 0.57 Å and 0.46 Å ranges in d spacing, were used for the analyses of 800 and 300 K data, respectively. The high angular region is enlarged and shown in the insets.

The charge-density distributions on the (0 1 0) plane, i.e., Pb-O plane, and the (0 2 0) plane, i.e., Ti-O plane, in cubic $PbTiO_3$ at 800 K are shown in Figs. 2(a) and 2(b), respectively. Their corresponding charge-density distributions in tetragonal $PbTiO_3$ at 300 K are shown in Figs. 2(c) and 2(d), respectively. The electron-density distributions around Pb and O in cubic $PbTiO_3$ are essentially isotropic on the Pb-O plane [see Fig. 2(a)]. The minimum charge density on the Pb-O bonding is $0.22e$ Å^{-3}. This is the same value as the background level. On the other hand, the electron-density distributions around Pb and O2 in tetragonal $PbTiO_3$ are quite anisotropic as shown in Fig. 2(c), i.e., extending toward O2 and Pb, respectively. The electron densities of Pb and O2 are found to be overlapped along the Pb-O2 direction in the tetragonal $PbTiO_3$. The minimum charge density on the shorter Pb-O2 bonding in Fig. 2(c) is charged up to $0.45e$ Å^{-3}. This means that the Pb-O bonding nature of the cubic phase is ionic, whereas that of the tetragonal phase is covalent. As a comparison, charge-density distributions of both cubic and tetragonal $BaTiO_3$ obtained by the same procedure are shown in Figs. 3(a)–3(d), corresponding to those of $PbTiO_3$ shown in Figs. 2(a)–2(d). Almost no overlapping electron distribution is observed between Ba-O(O2) bonding in both cubic and tetragonal $BaTiO_3$ showing an ionic bonding nature [see Figs. 3(a) and 3(c)]. The minimum charge density on the Ba-O bonding of cubic $BaTiO_3$ in Fig. 3(a) is $0.18e$ Å^{-3}. This value is unchanged on the Ba-O2 bondings of tetragonal $BaTiO_3$ in Fig. 3(c). Note that the electron density distributions around Ba and O2 are still isotropic on the Ba-O plane in tetragonal $BaTiO_3$. As for the interatomic distance in tetragonal $BaTiO_3$, there is not much difference between the experimentally obtained Ba-O distance of 2.80 Å and the theoretically calculated Ba-O distance of 2.82 Å, estimated based on the Shannon

TABLE I. Crystal parameters and structure parameters for $PbTiO_3$ refined by the Rietveld analysis. $R_I = 2.35\%$ and 1.72% for 800 and 300 K, respectively.

	Atom	x	y	z	u (10^{-2} Å^2)
800 K	Pb	0	0	0	3.71(1)
$Pm\bar{3}m$	Ti	0.5	0.5	0.5	1.65(4)
$a = 3.9692(1)$ Å	O	0.5	0.5	0	2.76(9)
300 K	Pb	0	0	0.1206(6)	0.97(1)
$P4mm$	Ti	0.5	0.5	0.5773(4)	0.56(3)
$a = 3.9040(1)$ Å	O1	0.5	0.5	−0.0077(9)	1.05(9)
$c = 4.1575(1)$ Å	O2	0.5	0	0.5	1.20(8)

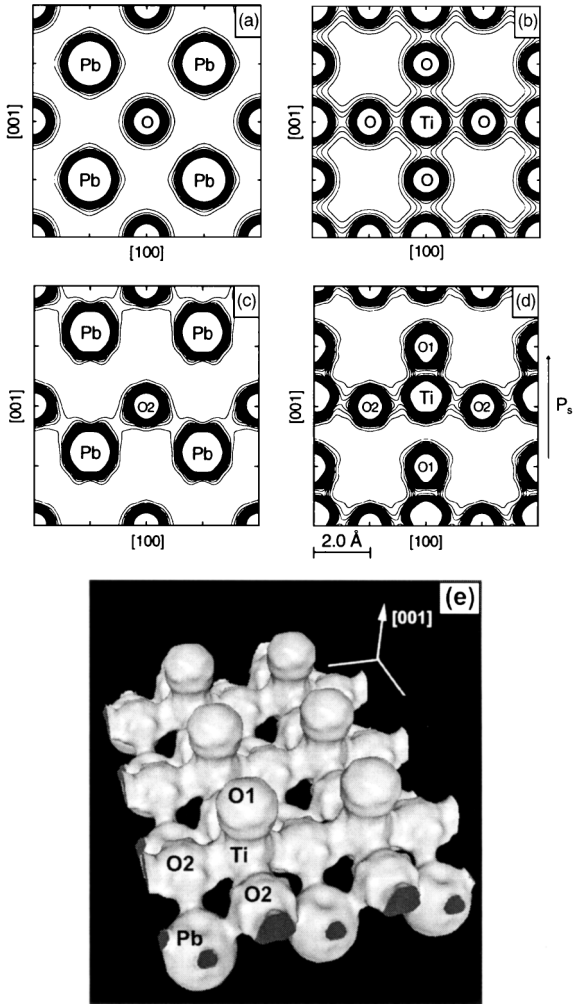

FIG. 2. MEM charge-density distributions of $PbTiO_3$; (a) and (b) cubic phase at 800 K, (c) and (d) tetragonal phase at 300 K. The left and right columns show the Pb-O plane and Ti-O plane, respectively. The contour lines are drawn from $0.4e$ Å^{-3} with $0.2e$ Å^{-3} intervals. (e) equicontour ($0.4e$ Å^{-3}) charge-density map of a two-dimensional covalent-bonding layered structure of $PbTiO_3$ at 300 K.

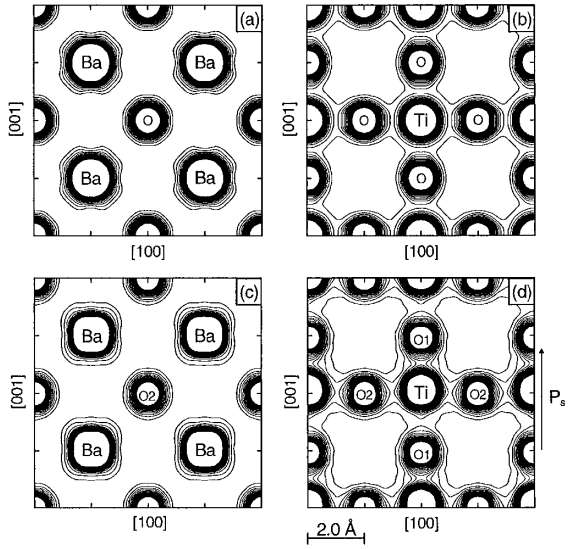

FIG. 3. MEM charge-density distributions of $BaTiO_3$; (a) and (b) cubic phase at 573 K, (c) and (d) tetragonal phase at 300 K. The left and right columns show the Ba-O plane and the Ti-O plane, respectively. The contour lines are drawn from $0.4e$ Å^{-3} with $0.2e$ Å^{-3} intervals. The data up to 62.8° in 2θ, which corresponds to the 0.48 Å ranges in d spacing, were used for both the analyses of 573 and 300 K data.

and Prewitt (S-P) ionic radii model [18,19]. On the other hand, a significant difference between the Pb-O distances of 2.51 Å (experiment) and 2.69 Å (S-P radii model) is found in tetragonal $PbTiO_3$. This suggests that the Pb-O bond in tetragonal $PbTiO_3$ cannot be interpreted by a simple ionic model. The present work gives the direct experimental evidence for existence of the Pb-O orbital hybridization in tetragonal $PbTiO_3$. This is high contrast to the almost ionic character of the bonding nature of the Ba-O bondings in tetragonal $BaTiO_3$. These differences are consistent with the theoretical predictions [5,6] and, thus, should be related to the difference of ferroelectric behavior between $PbTiO_3$ and $BaTiO_3$.

Two Ti-O1 bonding natures along the [001] direction in the tetragonal phase ought not to be identical due to the displacement of the Ti atom from the center of the oxygen octahedra along the [001] direction. The inequality of this bond nature is clearly seen in Figs. 2(d) and 3(d) when they are compared with the Ti-O bonding nature of the cubic phase in Figs. 2(b) and 3(b), respectively. The Rietveld analysis shows a very large difference of bond lengths between the O1-Ti and the Ti-O1 bonds in tetragonal $PbTiO_3$; the difference is 0.706 Å. The MEM analysis shows that the minimum charge density on the longer Ti-O1 bonding in tetragonal $PbTiO_3$ is extremely low as $0.22e$ Å^{-3}, the same level as the background level, while that on the shorter Ti-O1 bonding in tetragonal $PbTiO_3$ is considerably high as $1.25e$ Å^{-3}. The minimum charge density on the Ti-O2 bonding, perpendicular to the [001] direction, is $0.83e$ Å^{-3} in tetragonal $PbTiO_3$, which is almost the same as that of the Ti-O bonding in cubic $PbTiO_3$, $0.90e$ Å^{-3}. These facts suggest that the O1 atom moves also closer to a pairing Ti atom. Such a pairing of a Ti atom with an O1 atom along the [001] direction is surely associated with the pairing Pb atom with O2 atoms during the ferroelectric phase transition in $PbTiO_3$.

Turning our attention to the covalent network, we may say that tetragonal $PbTiO_3$ forms a layered structure of a two-dimensional network of covalent bonding, consisting of the Ti-O_5 pyramid strongly combined with the Pb-O bond. The equidensity surface of MEM charge densities for such a two-dimensional network is shown in Fig. 2(e) at the equicontour level of $0.4e$ Å^{-3}. The layer is perpendicular to the [001] direction, which may affect the coherent length on x-ray diffraction, e.g., the profile of the (002) reflection was 1.6 times as broad as the (200) reflection. This suggests that static stacking of the layers along the [001] direction is disarranged, presumably due to the two dimensionality caused by the particular bonding nature of tetragonal $PbTiO_3$.

The number of electrons around each atom can be computed in the charge-density distributions obtained by the MEM analysis. The counting region is the inside surrounded by a minimum charge-density surface that separates the atom from its neighbors. It was found that the number of electrons around Pb in tetragonal $PbTiO_3$ increased from 80.0(3)e to 80.9(3)e by 0.9e associated with the cubic-tetragonal phase transition, whereas the number of electrons around O2 decreased from 9.4(3)e to 9.0(3)e by 0.4e. It should be noted that the number of the electrons increased in Pb is approximately equal to the total number of electrons decreased in two O2 atoms. In the unit cell, there exist two equivalent O2 atoms, which are both combined with one Pb atom to form the Pb-O2 covalent bondings in the tetragonal $PbTiO_3$. We consider that such a charge transfer, corresponding to approximately one electron on Pb, is caused by the cubic-tetragonal phase transition, to influence the ferroelectric properties of $PbTiO_3$. With regard to the O1-Ti-O1 bondings in $PbTiO_3$, the numbers of electrons around O1 and Ti were almost unchanged, as 19.8(4)e (Ti) and 9.4(3)e (O) for cubic $PbTiO_3$; 19.6(4)e (Ti) and 9.4(3)e (O1) in tetragonal $PbTiO_3$. This result suggests that the numbers of electrons around Ti and O1 preserve a balance of total charge although the covalency inclines heavily toward the shorter Ti-O bond in tetragonal $PbTiO_3$. In the case of $BaTiO_3$, the numbers of electrons around constituent atoms computed by the same way is found to be almost unchanged through the cubic-tetragonal phase transition. They are 54.2(3)e for Ba, 19.9(3)e for Ti, and 9.3(3)e for O in cubic $BaTiO_3$, and 54.1(3)e for Ba, 20.1(4)e for Ti, 9.6(3)e for O1, and 9.1(3)e for O2 in tetragonal $BaTiO_3$.

The ionic state of atoms in tetragonal $PbTiO_3$ is easily estimated by subtracting the atomic number from the number of electrons around atoms: $+1.1$ for Pb, $+2.4$ for Ti, -1.4 for O1, and -1.0 for O2. This result provides an instructive contrast to the theoretical values of $+2$ (fixed) for Pb, $+2.89$ for Ti, and -1.63 for O (assumed all the same) in tetragonal $PbTiO_3$ [5]. We have found that the ionic state of Pb in $PbTiO_3$ changes from $+2.0$ to $+1.1$ through the cubic-tetragonal phase transition. The spontaneous polarization of the tetragonal $PbTiO_3$ can also be calculated from these ionic states and the displacements of cation sublattice relative to oxygen octahedron to be 0.33 C m^{-2}, which is smaller than the spontaneous polarization obtained by the measurement of a dielectric hysteresis loop, e.g., 0.75 [2] and 0.57 C m^{-2} [20]. In the present calculation, we take no account of the polarization related to the nucleus position that is unable to be determined by x-ray diffraction. The spontaneous polarization of tetragonal $BaTiO_3$ can also be estimated in the present charge-density study as 0.10 C m^{-2}, which is also smaller than the value by other experimental studies, 0.25 C m^{-2} [21].

The present study revealed the peculiar bonding nature of tetragonal $PbTiO_3$ on the basis of electron charge-density analysis by MEM. The further systematic charge-density study of other perovskite oxides shall give information essential for a better understanding of ferroelectric properties and for designing novel materials based on the orbital physics.

We thank H. Akamine for his experimental help at SPring-8. We also thank Professor Yasuhiko Fujii and Professor Tunetaro Sakudo for their helpful discussions. The experiment at SPring-8 has been carried out under the Program No. 2000B0377.

*To whom all correspondence and requests for materials should be addressed.
Email address: kuroiwa@science.okayama-u.ac.jp

[1] For example, see M. E. Lines and A. M. Glass, *Principles and Applications of Ferroelectrics and Related Materials* (Clarendon, Oxford, 1979).
[2] V. G. Gavrilyachenko, R. I. Spinko, M. A. Martynenko, and E. G. Fesenko, Sov. Phys. Solid State **12**, 1203 (1970).
[3] G. Shirane, R. Pepinsky, and B. C. Frazer, Acta Crystallogr. **9**, 131 (1956).
[4] R. E. Cohen and H. Krakauer, Phys. Rev. B **42**, 6416 (1990).
[5] R. E. Cohen, Nature (London) **358**, 136 (1992).
[6] R. E. Cohen and H. Krakauer, Ferroelectrics **136**, 65 (1992).
[7] G. Saghi-Szabo, R. E. Cohen, and H. Krakauer, Phys. Rev. Lett. **80**, 4321 (1998).
[8] W. Zhong, D. Vanderbilt, and K. M. Rabe, Phys. Rev. B **52**, 6301 (1995).
[9] A. V. Postnikov, T. Neumann, G. Borstel, and M. Methfessel, Phys. Rev. B **48**, 5910 (1993).
[10] E. Nishibori, M. Takata, K. Kato, M. Sakata, Y. Kubota, S. Aoyagi, Y. Kuroiwa, M. Yamakata, and N. Ikeda, Nucl. Instrum. Methods Phys. Res., Sect. A **467–468**, 1045 (2001).
[11] M. Sakata and M. Sato, Acta Crystallogr. Sect. A **46**, 263 (1990).
[12] H. M. Rietveld, J. Appl. Crystallogr. **2**, 65 (1969).
[13] M. Takata, B. Umeda, E. Nishibori, M. Sakata, Y. Saito, M. Ohno, and H. Shinohara, Nature (London) **377**, 46 (1995).
[14] M. Takata, E. Nishibori, M. Sakata, M. Inakuma, E. Yamamoto, and H. Shinohara, Phys. Rev. Lett. **83**, 2214 (1999).
[15] C.-R. Wang, T. Kai, T. Tomiyama, T. Yoshida, Y. Kobayashi, E. Nishibori, M. Takata, M. Sakata, and H. Shinohara, Nature (London) **408**, 426 (2000).
[16] Y. Kubota, M. Takata, M. Sakata, T. Ohba, K. Kifune, and T. Tadaki, J. Phys. Condens. Matter **12**, 1253 (2000).
[17] M. Takata, E. Nishibori, K. Kato, M. Sakata, and Y. Moritomo, J. Phys. Soc. Jpn. **68**, 2190 (1999).
[18] R. D. Shannon and C. T. Prewitt, Acta Crystallogr. Sect. B **25**, 925 (1969).
[19] R. D. Shannon, Acta Crystallogr. Sect. A **32**, 751 (1976).
[20] J. P. Remeika and A. M. Glass, Mater. Res. Bull. **5**, 37 (1970).
[21] W. J. Merz, Phys. Rev. **91**, 513 (1953); S. H. Wemple, M. Didomenico, Jr., and I. Camlibel, J. Phys. Chem. Solids **29**, 1797 (1968).